Granular Base Materials Subject to Repeated Loading Along Constant Stress Increment Ratio Path

S-C. R. Lo
B.Sc., Ph.D., M.I.E.Aust
Senior Lecturer, University College, The University of New South Wales
K. Chen
B.E., M.Eng., Ph.D.
Senior Engineer, Golder Associates, Cairns, Australia

Summary The responses of three granular base materials were studied by cyclic triaxial tests along constant stress increment ratio paths. The test results showed that the path followed during cyclic loading had a significant influence on the strain responses. A parameter referred to as the Proximity Index was found to be important in influencing the behaviour during cyclic loading. Provided the value of the Proximity Index is less than 0.7, the strain responses can be well modelled by a Cross-Anisotropic Elastic model. However, the elastic stiffness parameters were correlated to both the number of loading cycles and the mean stress.

1. INTRODUCTION

The introduction of analytically based pavement design procedures (AUSTROADS 1992, AASHTO 1993), sometimes referred to as "mechanistic design", led to strong interest in characterising the responses of granular base or sub-base materials subject to cyclic loading. These materials are collectively referred to as GB materials in this paper. Laboratory studies on the response of GB materials subject to cyclic loading have been based mainly on Conventional Cyclic Triaxial (CCT) tests where the confining pressure is maintained constant during application of cyclic loading in the axial direction. In these tests, the stiffness of GB materials under cyclic loading is commonly characterized by a resilient modulus, M_R, defined by Eqn (1) below (Hicks and Monosmith 1971).

$$M_R = \frac{\Delta q}{\Delta \varepsilon_a} \tag{1}$$

where Δq is the repeated deviator stress and $\Delta\varepsilon_a$ is the recoverable or resilient axial strain. Since the cell pressure in a CCT test is constant, M_R is in fact the Young's modulus, E, in the context of an elastic analysis. The test conditions of CCT testing are quite different from the stress changes experienced by a "typical" GB element of a pavement system during a wheel pass. The initial (ambient) stress of a GB element is low, and all stress components will vary simultaneously during a wheel pass (Brown 1996, O'Reilly and Brown 1992). Since a GB material is a geo-material, its stress–strain behaviour is highly non-linear. Hence, M_R or E is simply a parameter used to "linearise" the relationship between stress and strain changes and the question of conducting cyclic triaxial tests with more representative stress paths has to be addressed.

Simultaneous changes of all stress components can be approximated by triaxial testing along a constant stress increment ratio path (Lo and Lee 1990) defined by Eqn (2).

$$\frac{\Delta \sigma_r}{\Delta \sigma_a} = r \tag{2}$$

where $\Delta\sigma_a$ and $\Delta\sigma_r$ are the changes in axial and radial stresses respectively, and r is fixed at a prescribed value during a cyclic triaxial test. In compressive loading mode, the axial direction is the major principal stress direction. A CCT test is a particular case of Eqn (1) with r = 0.

This paper presents a testing system that can conduct, reliably, cyclic triaxial testing along a wide spectrum of constant stress increment ratio paths. Representative test results for three GB materials are presented. A range of factors that affect the strain responses were examined. Attempts were made in modelling the relationship between stress and strain changes during a loading cycle by isotropic and anisotropic elasticity. The relationship between residual strain and recoverable strain was also investigated. Since pore water pressure (suction) was not measured in this study, all interpretations were based on total stress.

2. TESTING SYSTEM

The cyclic Triaxial Testing System is schematically shown in Figure 1 and detailed in Lo & Chen (1998). Accurate measurement of stress and strain was achieved by

- an internal load cell
- two axial and one radial Hall Effect (HE) transducers mounted directly on the sample

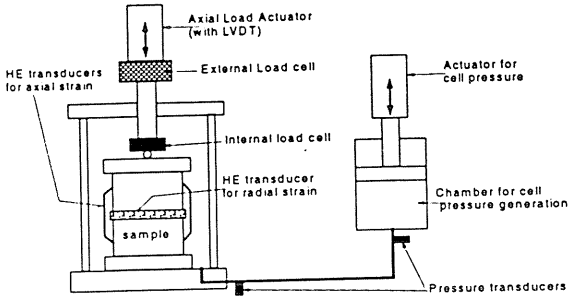

Figure 1. Cyclic triaxial testing system.

In cyclic loading, the discrepancy between internal and external load measurements could attain 20% (Lo & Chen 1998). The discrepancies between external and local axial strain measurements were even more considerable, 50 to 100% (Lo & Chen 1998), because of small strain level.

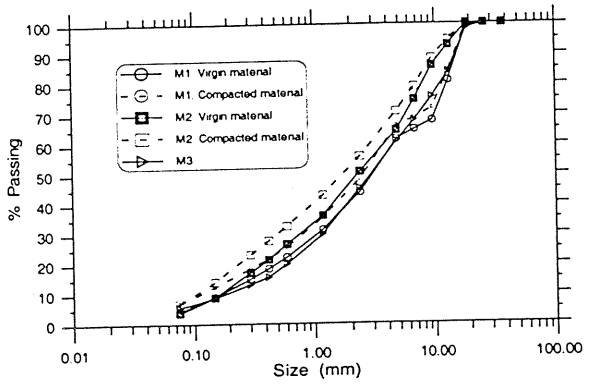

Figure 2. Grading curves.

3. TESTING METHODS

The triaxial samples, which were 100 mm diameter by 200 mm height, were prepared by dynamic compaction with an input energy of 894 kJ/m^3. The procedure for eliminating sample disturbance during the transfer of the compacted sample to the triaxial cell was detailed in Lo & Chen (1998).

It was recognised that even highly polished platen can impose significant restraint to radial deformation (Chu, Lo & Lee 1992). Such non-uniform radial, although not visible to the naked eye at low strain, is still significant for a sample with a height to diameter ratio of two (Kim, Drescher and Newcomb 1997). To reduce platen restraint to a minimal value, the free-end technique developed originally for monotonic triaxial testing was adapted to cyclic triaxial testing of GB materials (Lo & Chen 1998). The membrane was coated with liquid rubber (Lo et al 1989) to prevent puncturing of the membrane during cyclic loading.

4. TESTING PROGRAM

4.1 Material Tested

Three materials, referred to as M1, M2, and M3, were tested. All three materials were crushed rock with some fines. The average moisture contents and densities achieved were listed in Table 1. The grading curves of the three materials are shown in Fig. 2. The difference between the "before compaction" and "after compaction" grading curves was due to particle breakage induced by compaction, and this effect was most significant for material M2. For material M3, only one grading curve was shown because particle breakage did not occur.

Table 1. Soil parameters.

Material	Moisture Content (%)	Density (t/m^3)
M1	6	2.241
M2	6	2.264
M3	5	2.307

4.2 Constant Stress Increment Ratio Paths

A constant stress increment ratio path is illustrated in Fig. 3. Point "O" corresponds to the initial (or ambient) stress state prior to the application of cyclic loading. The path for cyclic loading followed "AB". Point B may be different from point "O" because of imperfection in control at very low stress level.

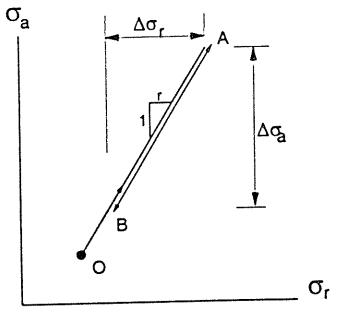

Figure 3. Constant stress increment ratio path.

The change in stress along "AB" is referred to as cyclic stress which consists of two components $\Delta\sigma_a$ and $\Delta\sigma_r$ defined by Eqns (3) and (3a) below and illustrated in Fig. 3.

$$\Delta\sigma_a = \sigma_a(A) - \sigma_a(B) \quad (3)$$

$$\Delta\sigma_r = \sigma_r(A) - \sigma_r(B) \quad (3a)$$

Only compression tests were conducted. Three types of tests along constant stress increment ratio paths were conducted.

a) CCT tests: These tests were conventional cyclic triaxial defined by r = 0, ie $\Delta\sigma_r = 0$.

b) HCT tests: These tests were defined by r = 1, (ie $\Delta\sigma_a = \Delta\sigma_r$). Such tests were conducted by cycling the confining stress under zero axial load.

c) *SPCT tests:* These tests, the focus of this paper, were defined by a non-zero and non-unity r value. A range of r values were covered to allow a systematic study of the influence of r on stress strain behaviour. SPCT tests were subdivided into three different series as explained below.

- Δq-series tests: the stress path was defined by $\sigma_{r0} \approx 10$ kPa and $\Delta q \approx 240$ kPa, where σ_{r0} is the initial confining stress. The r value covered in this test series was in the range of 0.1 to 0.5.
- $\Delta\sigma_a$-series tests: the stress path was defined by $\sigma_{r0} \approx 10$ kPa and $\Delta\sigma_a \approx 240$ kPa. The r value covered in this test series was in the range of 0.2 to 0.6
- p-series tests: These tests were conducted with $\Delta\sigma_a > 0$ and $\Delta\sigma_r < 0$; and hence, the $r < 0$.

All cyclic triaxial tests were conducted in a stress controlled mode. Note that Δq and $\Delta\sigma_a$ series tests may start from a very low σ_{r0} value of about 10 kPa.

5. TEST RESULTS

The stress and strain reported were based on internal and local measurements. The test results are the true behaviour of GB materials even at small number of loading cycles. The stress changes along "AB" (see Fig. 3), $\Delta\sigma_a$ and $\Delta\sigma_r$, are collectively denoted by $\Delta\sigma$. The n-th load cycle is defined by the n-th application of $\Delta\sigma$. Hence, the first loading cycle (n = 1) corresponds to virgin loading followed by unloading. Thus, the data corresponding to n = 1 were excluded in this paper because stress–strain response in virgin loading may be dominantly plastic. The notations $\Delta\varepsilon_a(n)$ and $\Delta\varepsilon_r(n)$ are used to denote the changes in axial and radial strain respectively during the n-th application of $\Delta\sigma$. As such, $\Delta\varepsilon_a(n)$ and $\Delta\varepsilon_r(n)$ can be dependent on the number of loading cycles. The following stress and strain parameters were used in this paper.

$$q = \sigma_a - \sigma_r = \text{deviator stress} \quad (4)$$

$$p = (\sigma_a + 2\sigma_r)/3 = \text{mean stress} \quad (4a)$$

$$\varepsilon_q = 2(\varepsilon_a - \varepsilon_r)/3 = \text{deviatoric strain} \quad (4b)$$

$$\varepsilon_v = (\varepsilon_a + 2.\varepsilon_r) = \text{volumetric strain} \quad (4c)$$

The use of ($\Delta\varepsilon_q$, $\Delta\varepsilon_v$) is considered to be more appropriate than ($\Delta\varepsilon_a$, $\Delta\varepsilon_r$) in representing the strain responses of SPCT tests.

5.1 Strain Responses

CCT test results were reported in Lo & Chen (1998). Some typical results on evolution of cyclic deviatoric strains ($\Delta\varepsilon_q$) and cyclic volumetric strains ($\Delta\varepsilon_v$) of SPCT tests are presented in Figs. 4-5. The tests were Δq-series SPCT tests, ie Δq kept at a nominal value of 240 kPa, but with the stress increment ratio, r, varied between tests. The following characteristics were observed.

- Both $\Delta\varepsilon_q$ and $\Delta\varepsilon_v$ changed with the number of loading cycles
- The stress increment ratio, r, affected the evolution of both $\Delta\varepsilon_q$ and $\Delta\varepsilon_v$.

The above observations were also applicable for the σ_a-series of SPCT tests.

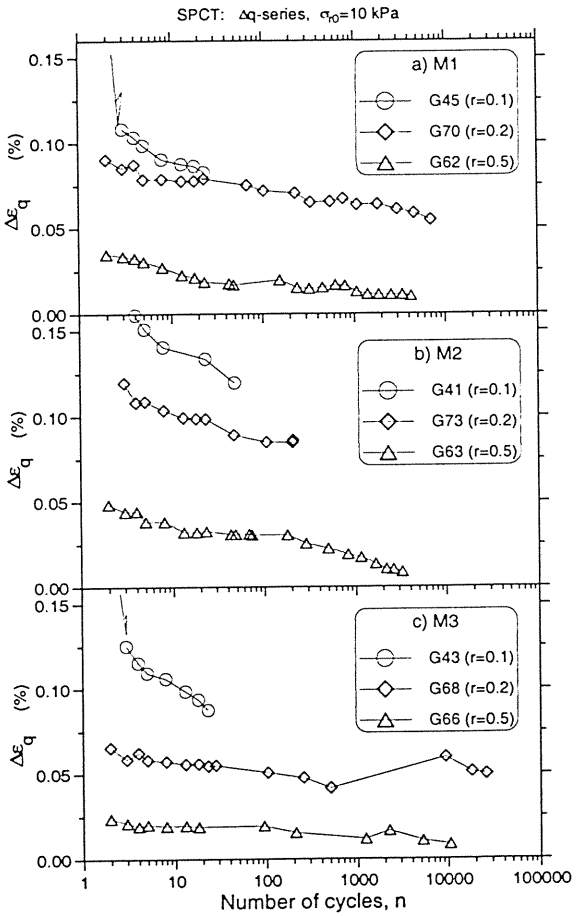

Figure 4. Cyclic deviatoric strain.

Typical accumulation of residual strains, for Δq-series SPCT tests are presented in Fig. 6 for deviatoric residual strain, ε^r_q , and in Fig. 7 for volumetric residual strain, ε^r_v. The following characteristics were observed.

- Both ε^r_q and its rate of accumulation are dependent on the stress increment ratio, r. A lower r value led to higher ε^r_q value.
- Both ε^r_v and its rate of accumulation are

dependent on r. A higher r value led to higher ε^r_v value. For r = 0.1, the rate of accumulation of ε^r_v can be dilative.

- For r = 0.1, ε^r_q increased rapidly with number of loading cycles, which then led to failure.

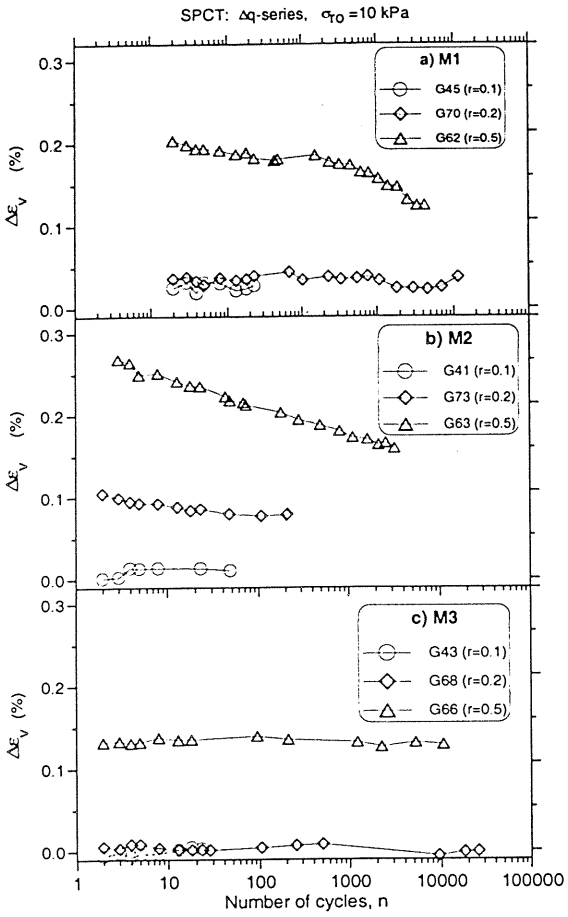

Figure 5. Cyclic volumetric strain.

5.2 Proximity Index

The test results showed that the strain responses depended on the stress path as defined by r, the value of Δq, and the value of σ_{ro}. However, a parameter ζ, defined by Eqn (5) below and illustrated in Fig. 8 was found to be relevant in classifying the overall behaviour of GB materials subject to cyclic loading.

$$\zeta = \frac{q_A}{M_f \cdot p_A + q_{of}} \leq 0.7 \qquad (5)$$

where M_f and q_{of} are the strength parameters used to define (and linearize) the failure surface (Fig. 8). ζ is referred to as the Proximity Index. ζ = 0 for hydrostatic loading and ζ = 1 at failure. Provided ζ < 0.7, significant plastic behaviour such as dilatancy or run off in deviatoric strain will not occur for all three materials, irrespective of the test conditions.

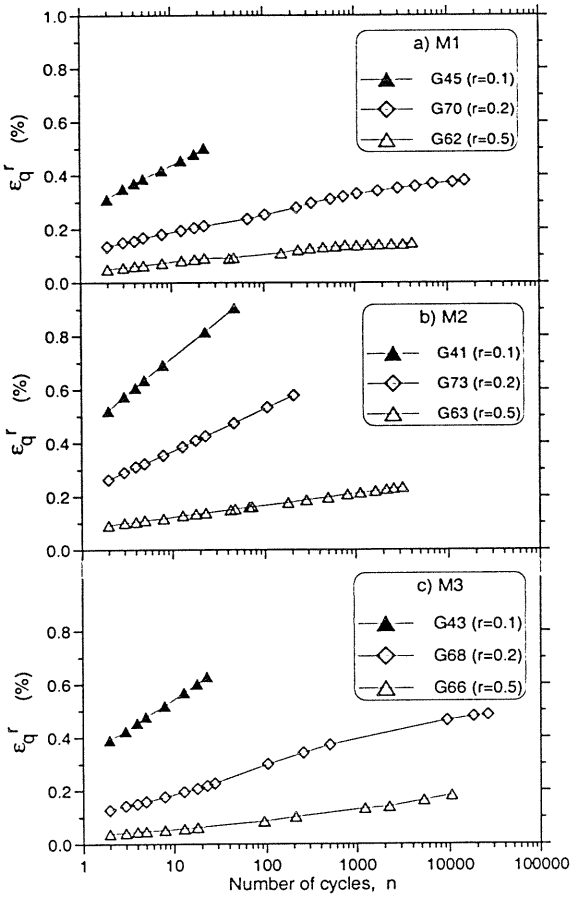

Figure 6. Residual deviatoric strain.

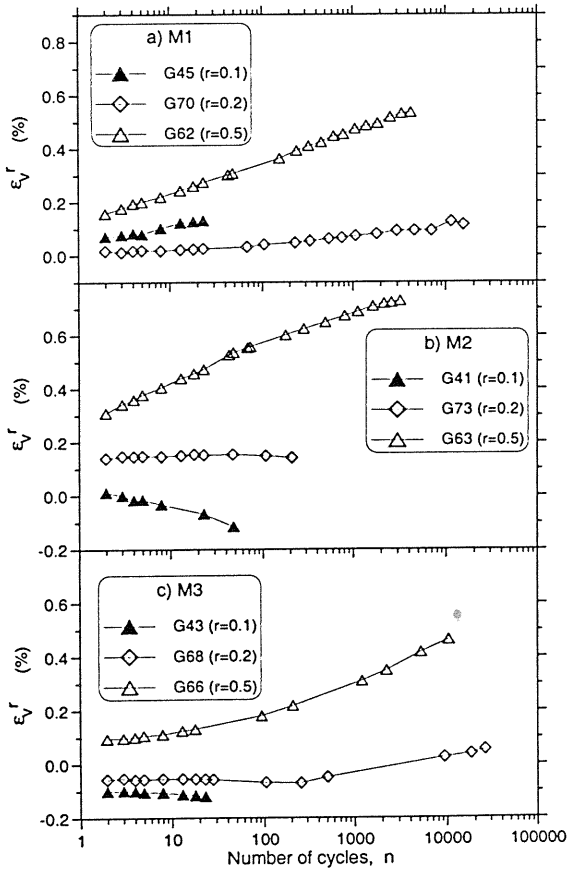

Figure 7. Residual volumetric strain.

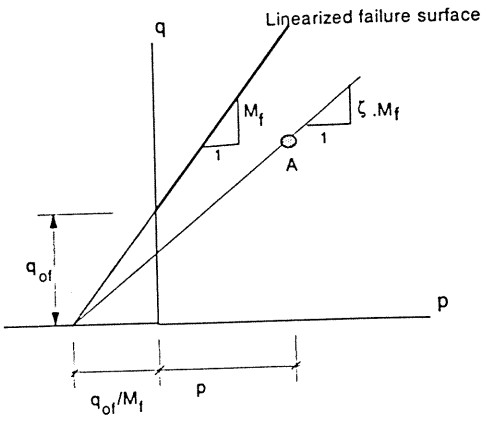

Figure 8. Proximity Index.

6. ELASTIC MODELLING

This section attempts to model the observed strain response during cyclic loading by an isotropic or anisotropic elastic model. As such, only data from tests that satisfied the condition of $\zeta < 0.7$ were used in this section. If isotropic elasticity is assumed, then a representative Young's modulus (E) and Poisson's ratio (ν) for the n-th loading cycle should be computed from Eqns (6), (7) below

$$\nu(n) = \frac{\Delta\sigma_a.\Delta\varepsilon_r(n) - \Delta\sigma_r.\Delta\varepsilon_a(n)}{-(\Delta\sigma_a + \Delta\sigma_r)\Delta\varepsilon_a(n) + 2.\Delta\sigma_r.\Delta\varepsilon_r(n)} \quad (6)$$

$$E(n) = \frac{\Delta\sigma_a - 2.\nu(n).\Delta\sigma_r}{\Delta\varepsilon_a(n)} \quad (7)$$

where (n) indicates that it is specific to the n-th loading cycle. If $\Delta\sigma_r = 0$, Eqns (6) and (7) yield $E = \Delta\sigma_a/\Delta\varepsilon_a = \Delta q_a/\Delta\varepsilon_a = M_R$.

For SPCT tests, both $\Delta\sigma_a$ and $\Delta\sigma_r$ are non-zero. The interpreted isotropic elasticity parameters for material M1 (n = 5 to 25) are presented in Fig. 9. To minimize the influence of mean stress, p, on the E value, only test data with a p_{max} value in the range of 200 to 320 kPa were included for $r \geq 0$ tests, where subscript "max" denotes maximum value during a loading cycle. The data points for r = -0.5 correspond to a constant p test with p_{max} = 160 kPa. The wide range of E value obtained, as explained in detail by Chen (1997), cannot be explained by the influence of mean stress value, and hence must be attributed to the effect of stress path as defined by the stress increment ratio, r. But elastic parameters have to be path independent in order to ensure mathematical consistency. The most significant finding is the Poisson's ratio, ν, can exceed 0.5 or become negative. This is physically and computationally inadmissible. The negative Poisson's ratio does not mean the sample contracts radially under application of $\Delta\sigma_a$. Rather, it is the consequence of fitting the as measured and non-zero values of $\Delta\varepsilon_a$, $\Delta\varepsilon_r$. $\Delta\sigma_a$ and $\Delta\sigma_r$ by the isotropic elastic equations. This implies that isotropic elasticity cannot be used to consistently fit SPCT test results.

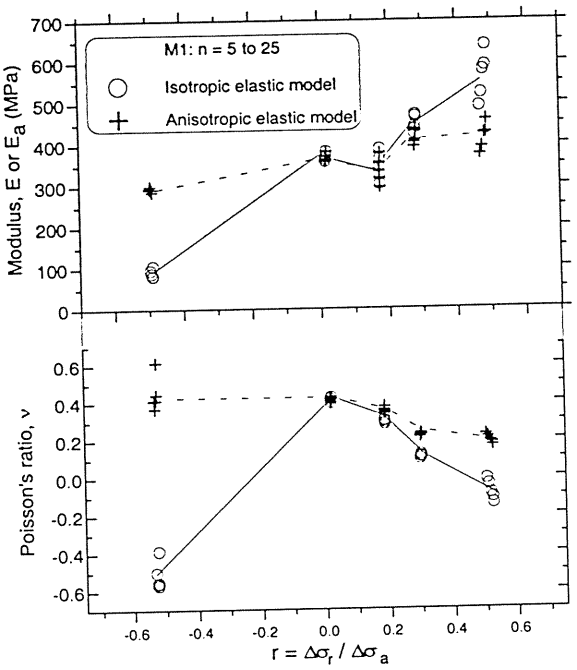

Figure 9. Elastic parameters.

Alternatively, a cross anisotropic elastic model expressed as Eqns (8), (9) below for axi-symmetric condition can be used to fit the as measured cyclic stress strain responses.

$$\Delta\varepsilon_a = \left(\frac{1}{E_a}\right).\Delta\sigma_a - \frac{2\nu_a}{E_a}.\Delta\sigma_r \quad (8)$$

$$\Delta\varepsilon_r = \left(\frac{-\nu_a}{E_a}\right).\Delta\sigma_a + \frac{(1-\nu_r)}{E_r}.\Delta\sigma_r \quad (9)$$

where E_a and E_r are the Young's moduli in the axial and radial directions respectively, ν_a is the Poisson's ratio for the axial-radial plane and ν_r is the Poisson's ratio for the plane containing the radial directions only. The use of Eqns (8) and (9) is only meaningful if the material stiffness is anisotropic. This hypothesis can be investigated by conducting HCT tests and measuring the stiffness ratio, SR(n), defined by Eqn (10) below.

$$SR(n) = \Delta\varepsilon_r / \Delta\varepsilon_a \quad (10)$$

The as measured stiffness ratios (see Table 2) in general differed from unity, thus implying stiffness anisotropy. In order to deduce the anisotropic

elastic parameters from the cyclic triaxial tests, the following assumptions were made.

- The stiffness ratio measured in HCT tests were applicable to other test conditions
- $\nu_a = \nu_r$

Table 2. Stiffness parameters.

Material	Stiffness Ratio	K	θ
M1	1.8	280	0.65
M2	1.4	280	0.55
M3	2.0	270	0.45

As discussed in Chen (1997), these assumptions were reasonable and tenable provided only compression mode cyclic loading was considered. These two assumptions implied that the ratio of Young's modulus in the two directions was independent of n, but E_a and E_r can vary with n. The interpreted anisotropic elastic parameters for M1 (with n = 5 to 25) are plotted in Fig. 9. Both E_a and ν were only slightly affected by r, and the value of ν was always reasonable and admissible, with the exception of one data point for r = –0.5. Since CCT data were included in the plot, the above results appear to suggest that E_a could be measured with CCT tests. However, such an inference has to be treated with caution because only CCT tests with p_{max} values similar to the SPCT tests were plotted. A detailed study of all test data revealed a definite correlation between E_a and p_{max} as expressed by Eqn (11).

$$E_a(1000+) = K\left(p_{max}/p_a\right)^{\theta} \qquad (11)$$

where E_a (1000+) is the E_a value corresponding to n ≥ 1000, p_{max} is the maximum mean stress in a loading cycle, p_a is the standard atmospheric pressure in consistent units, and K and θ are material constants as listed in Table 2. Eqn (11) implies that, when n > 1000, the change in E_a with n is minimal. The values of K and θ for the three materials were similar. This implies that the E_a(1000+) values of the three materials, after normalisation with p_{max}, only differed slightly. For n < 1000, the evolution of E_a with number of loading cycles was studied by plotting E_a/E_a(1000+) versus n. In view of the large number of data points, only the upper and lower bound curves for M1 and M2 are presented (Fig. 10). Note that E_a(1000+) was computed from Eqn (11) and hence values of E_a / E_a(1000+) could exceed unity because of prediction error. For a given material, the difference between the upper and lower bound curves at n ≈ 100 was still about 30%. This difference was even higher at lower n values. The data band for CTC tests were hatched. This hatched zone, however, was narrow compared with the range between the upper and lower bound curves. Hence, this range has to be attributed to the influence, the stress increment ratio, r, on the measured E_a value. The lower bound curve for M2 was different from M1. This implied that the influence of r on the evolution of E_a value with n was material dependent.

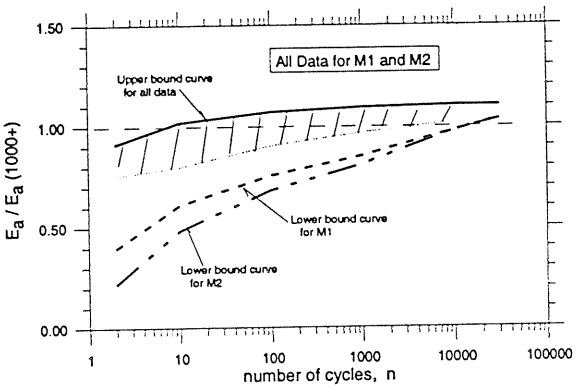

Figure 10. Evolution of E_a.

7. RESIDUAL STRAIN

The evolution of axial residual strain $\varepsilon_a^r(n)$ with loading cycle was studied with the residual strain function (RSF) defined by Eqn (12) below.

$$RSF(n) = \varepsilon_a^r(n) / \Delta\varepsilon_a(n) \qquad (12)$$

where (n) denotes the n-th load cycle. It is pertinent that the as measured value of recoverable strain (which varied with n) was used in calculating RSF. The RSR versus n relationship was examined in Fig. 11. Both CCT and SPCT tests data were included in the plot. For clarity, the upper and lower bound curves for all the data points for ζ < 0.7 were also plotted because of the very large number of tests and data points. For a given material, the data points were located within a narrow band irrespective of the test type and r value. However, there was some dependency on ζ. This can be illustrated from the data points corresponding to ζ > 0.7. For n >1000, however, the variation of recoverable strain with n was slight. The RSF-n correlation depends on the material type. At n = 1000, RSF was in the range of 4 to 5 for M1 but took a significantly lower value in the range of 6 to 8 for M2.

8. CONCLUSIONS

The significance of conducting cyclic triaxial tests along constant stress increment paths was addressed. The use of a non-zero stress increment ratio (r > 0.1) enables the application of cyclic loading from a low and realistic initial cell pressure.

The stress increment ratio had a significant influence on both the strain changes during a loading cycle, and the accumulation of residual strain. The Proximity Index defined by Eqn (5) is an important parameter in determining the behaviour pattern during cyclic loading. Significant plastic behaviour could occur if the Proximity Index exceeded 0.7.

Stress Path Cyclic Triaxial test data ($r \neq 0$) could not be consistently interpreted by the isotropic elastic model. However, a cross anisotropic elastic model could be used to consistently interpret the stress and strain data from all tests conducted with a Proximity Index less than 0.7.

The cyclic stiffness was dependent on the number of loading cycles, but tended to an asymptotic value, $E_a(1000+)$, when the number of loading cycles exceeded 1000. $E_a(1000+)$ of the three materials, when normalised with p_{max}, were similar. This implied that pre-conditioning, a common practice in measurement of cyclic stiffness in pavement engineering, yields stiffness values that may not be a good indicator of material performance.

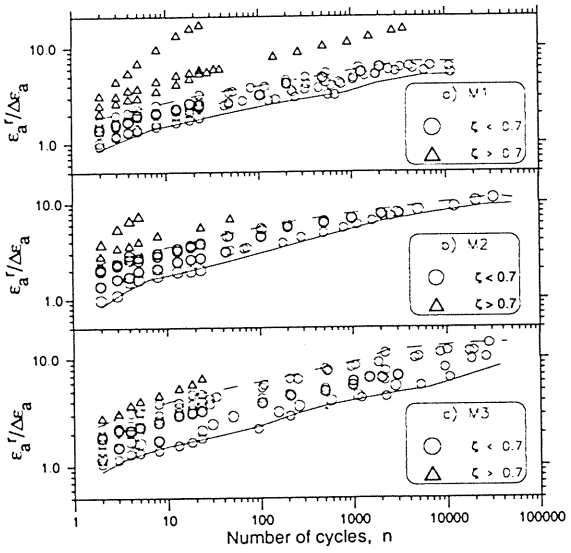

Figure 11. Residual strain function

The relationship between residual axial strain and recoverable axial strain was only slightly affected by the test conditions and the value of r, provided the Proximity Index was less than 0.7. This gave support to the current practice of assessing long term rutting from resilient deformation. The relationship between recoverable strain and residual strain depended on the material type. This implied that the development of residual strain was a good indicator of material performance.

9. ACKNOWLEDGEMENT

The second author was supported by a scholarship sponsored by Boral Resources Pty Ltd while conducting his PhD research at the University College, UNSW. The opinions expressed in this paper, however, were solely those of the authors.

10. REFERENCES

AASHTO (1993). Guide for the design of pavement structures, *American association of State Highway and Transportation*. 324p.

AUSTROADS (1992). A guide to the structural design of road pavement, *AUSTROADS*, Syd, Australia. 157p.

Brown, S.F. (1996).Soil mechanics in pavement engineering, Rankine Lecture, *Geotechnique*, Vol. 46, No. 3, pp. 383-426.

Chen, K. (1997). Behaviour of pavement materials under cyclic loading. *PhD Thesis, University College, University of New South Wales*. 266p.

Chu, J., Lo, S-C.R. and Lee, I.K. (1992). Strain softening of a granular material in triaxial and multi-axial testing, *Proc 6th ANZ Conference in Geomechanics*, Christchurch, New Zealand, pp. 309-314.

Clayton, C.R.I. and Khatrush, S.A. (1986). A new device for measuring local strains on triaxial specimens, *Geotechnique*, Vol. 36, No. 4, pp. 593-597.

Hicks, R.G. and Monosmith, C.L. (1971). Factors influencing the resilient response of granular materials, *Highway Research Record No. 345*, pp. 15-31.

Kim, J.R., Drescher, A. and Newcomb, D.E. (1997). Rate sensitivity of an asphalt concrete in triaxial compression, *ASCE, J. of Civil Engr. Materials*, Vol. 9, No. 2, 76-85.

Lo, S-C.R., Chu, J. and Lee, I.K. (1989). A technique for reducing membrane penetration and bedding errors, *Geotechnical Testing Journal*, ASTM, Vol. 2, No. 4, pp.311-316.

Lo, S-C.R. and Lee, I.K. (1990). Response of granular soil along constant stress increment ratio path, *ASCE, J. of Geot. Engr.*, Vol. 116, No.3, pp. 355-376.

Lo S-C.R. and Chen K. (1998). Stiffness of granular base materials in repeated triaxial testing, *ARRB Journal, Vol.* 7, No.2, pp. 16-35.

O'Reilly, M.P. and Brown, S.F. (1992). Observations on the resilient shear stiffness of granular materials, *Geotechnique,* Vol. 42, No. 4, pp. 631-633.